JOURNAL OF OPTOELECTRONICS AND ADVANCED MATERIALS Vol. 9, No. 6, June 2007, p. 1671 – 1678

Section 6. Advanced processing and characterization / non-crystalline solids
Invited Paper

In-situ transmission electron microscopy: on moving dislocations and mobile grain boundaries

J. T. M. DE HOSSON*, W. SOER
Department of Applied Physics, Materials Science Centre and the Netherlands Institute for Metals Research, University of Groningen, Nijenborgh 4, 9747 AG Groningen, the Netherlands

This paper delineates the possibilities of utilizing in situ transmission electron microscopy to unravel dislocation-grain boundary interactions. In situ nanoindentation experiments have been conducted in TEM on ultrafine-grained Al and Al-Mg films with varying Mg contents. The observed propagation of dislocations is markedly different between Al and Al-Mg films, i.e. the presence of solute Mg results in solute drag, evidenced by a jerky-type dislocation motion with a mean jump distance that compares well to earlier theoretical and experimental results. The in situ indentation measurements confirm grain boundary motion as an important deformation mechanism in ultrafine-grained Al when it is subjected to a highly inhomogeneous stress field as produced by a Berkovich indenter. It is found that solute Mg effectively pins high-angle grain boundaries during such deformation. The mobility of low-angle boundaries is not affected by the presence of Mg.

(Received November 14, 2006; accepted April 26, 2007)

Keywords: Transmission electron microscopy, Moving dislocations, Mobile grain boundaries

1. Introduction

Microscopy in the field of materials science is generally devoted to linking microstructural observations to properties. However, the actual linkage between the microstructure studied by microscopy on one hand and the physical property of a material on the other hand is almost elusive. The reason is that various physical properties are determined by the collective behavior of defects rather than by the behavior of a single defect. For instance, there exists a vast amount of electron microscopy analyses concerned with post mortem observation of ex-situ deformed materials, which try to link observed patterns of defects to the mechanical property. However, in spite of the enormous effort that has been put in both theoretical and experimental work, a clear physical picture that can predict even one simple stress-strain curve based on these microscopy observations is still lacking.

Of course it has been realized for a long time that in the field of dislocations, disclinations and interfaces in materials, we are facing non-equilibrium effects. The defects determining mechanical performance are in fact not in thermodynamic equilibrium and their behavior is very much non-linear. This is a fundamental problem since adequate physical and mathematical bases for a sound analysis of these highly non-linear and non-equilibrium effects do not exist. Another (more practical) reason why a quantitative evaluation of the structure-property relationship of materials is hampered has to do with statistics. Metrological considerations of quantitative electron microscopy of crystalline materials pose some relevant questions to the statistical significance of the electron microscopy observations. In particular, in situations where there is only a small volume fraction of defects present or where there is a very inhomogeneous distribution, statistical sampling may be a problem.

For a long time, a major drawback of experimental and theoretical research in the field of dislocations and grain boundaries has been that most of the work has been concentrated on static structures. Obviously, the dynamics of moving dislocations and grain boundaries are more relevant to the deformation of metals. Nuclear spin relaxation methods in the rotating frame have been developed as a complementary tool for studying dislocation dynamics in metals [1]. A strong advantage of this technique is that it detects dislocation motion in the bulk of the material, in contrast to in situ transmission electron microscopy, where the behavior of dislocations may be affected by image forces due to the proximity of free surfaces. However, information about the local response of dislocations to an applied stress cannot be obtained by nuclear spin relaxation and therefore in situ transmission electron microscopy remains a valuable tool in the study of dislocation dynamics. Direct observation of dislocation-grain boundary interactions during indentation has recently become possible through in situ nanoindentation in a transmission electron microscope. In this paper, results obtained with this technique are presented, the results pertaining to the study of deformation mechanisms in Al and Al-Mg alloys with grain sizes of the order of a few hundred nanometers.

The recently developed technique of in situ nanoindentation in a transmission electron microscope [2-7] does not suffer from these limitations and allows for direct observation of indentation phenomena. Furthermore, as the indenter can be positioned on the specimen

accurately by guidance of the TEM, regions of interest such as particular crystal orientations or grain boundaries can be specifically selected for indentation. In situ nanoindentation measurements [7] on polycrystalline aluminum films have provided experimental evidence that grain boundary motion is an important deformation mechanism when indenting thin films with a grain size of several hundreds of nanometers. This is a remarkable observation, since stress-induced grain boundary motion is not commonly observed at room temperature in this range of grain sizes.

Results will be summarized on the indentation behavior of Al-Mg films and the effect of Mg on the deformation mechanisms described above. To this end, in situ nanoindentation experiments have been conducted on ultrafine-grained Al and Al-Mg films with varying Mg contents [8,9]. The classification "ultrafine-grained" in this respect is used for materials having a grain size of the order of several hundreds of nanometers. In this paper, the TEM observations are interpreted and related to quantitative load-displacement data, both directly from the in situ indentation experiments and indirectly through conventional ex situ nanoindentation on the same specimens.

2. Experimental procedure

In situ nanoindentation inside a TEM requires a special specimen stage designed to move an indenter towards an electron-transparent specimen on the optic axis of the microscope. The first indentation holder was developed in the late 1990s by Wall and Dahmen [2,3] for a high-voltage microscope at the National Center for Electron Microscopy (NCEM) in Berkeley, California. In the following years, several other stages were constructed at NCEM with improvements made to the control of the indenter movement but without a transducer dedicated to measuring load and displacement. In the work described in this paper, two stages were used: a homemade qualitative holder constructed at NCEM for a JEOL 200CX microscope [4] and a prototype quantitative holder developed at Hysitron (Hysitron, Inc., Minneapolis, MN) in collaboration with NCEM for a JEOL 3010 microscope. The latter holder is the first to accomplish in a TEM what is commonly referred to as depth-sensing indentation.

Certain design aspects of both holders are roughly the same. A piezoelectric tube allows high-precision movement of the tip in three dimensions, the indentation direction being perpendicular to the electron beam. Coarse positioning is provided by manual screw drives that move the indenter assembly against the vacuum bellows. The indenter itself is a Berkovich-type diamond tip, which is boron-doped in order to be electrically conductive in the TEM. The goniometer of the TEM provides a single tilt axis, so that suitable diffraction conditions can be set up prior to indentation.

In the case of the qualitative holder, the indenter tip is mounted directly to the piezo tube. The motion of the indenter into the specimen during indentation is accomplished by manual control of the voltage applied to the tube, which is recorded together with the TEM image. Since the compliance of the load frame is relatively high, the actual displacement of the indenter into the material depends not only on the applied voltage, but also to a certain extent on the response of the material. Consequently, this indentation mode is neither load- nor displacement-controlled. If the complex response of the piezo tube were fully known, the load could be calculated at any time during indentation from the motion provided by the piezo tube, the displacement of the indenter tip (which can be determined directly from the TEM image if in bright-field mode) and the compliance of the load frame [10,11].

The silicon ridge specimen geometry provides a means to investigate any material that can be deposited as a thin film onto the silicon substrate. Metals with a low atomic number such as aluminum are particularly suitable for this purpose, since films of these metals can be made to several hundreds of nanometers thickness and still be transparent at the cap of the wedge to electrons with typical energies of 200-300 keV, as schematically depicted in Fig. 1a. An example of a resulting TEM image is shown in Fig. 1b.

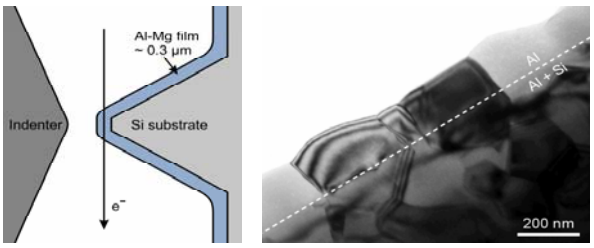

Fig. 1. (a) Schematic of in situ indentation setup. The deposited Al-Mg film is electron-transparent and accessible to the indenter at the tip of the Si wedge. (b) Typical bright - field image of a deposited film. The dashed line shows the top of the Si ridge.

3. Materials

The Al and Al-Mg films for the present investigation were deposited by thermal evaporation. The substrate was kept at 300 °C to establish a grain size of the order of the layer thickness, which was 200 to 300 nm for all specimens. After evaporation, the substrate heating was switched off, allowing the specimen to cool down to room temperature in approximately one hour. One pure Al film was prepared by evaporating a high purity (5N) aluminum source. Deposition of the Al-Mg alloy films was achieved by evaporating alloys with varying Mg contents. Since Al and Mg have different melting temperatures and vapor pressures, the Mg content of the deposited film is not necessarily equal to that of the evaporated material. Moreover, the actual evaporation rates depend on the quality of the vacuum and the time profile of the crucible temperature. The composition of the deposited alloy films was therefore determined by energy dispersive spectrometry (EDS) in a scanning electron microscope at

5 kV. The measured Mg concentrations of the four Al-Mg films prepared were 1.1, 1.8, 2.6 and 5.0 wt%.

Since the solubility level of Mg in Al is 1.9 wt% at room temperature [12], β' and β precipitates were formed in the 2.6 and 5.0 wt% Mg specimens due to the relatively long cooling time. The attainable image resolution in the indentation setup was not high enough to resolve these precipitates, being compromised by the thickness of the specimen and possibly by the fact that the electron beam travels very closely to the substrate over a large distance.

On each of the evaporated films, three to four in situ experiments were carried out with maximum depths ranging from 50 to 150 nm, using the indentation stage for the JEOL 200CX. The indentation rate, being controlled manually through the piezo voltage, was of the order of 5 nm/s. Conventional nanoindentation measurements were carried out ex situ on the same films away from the wedge. As in the in situ experiments, a pyramidal Berkovich tip was used. Load-controlled indentations were executed to maximum depths of 50, 100 and 150 nm at a targeted strain rate of 0.05 s^{-1}, defined as loading rate divided by load. At this strain rate the indenter velocity during loading was of the order of 2 nm/s, which is comparable to the in situ measurements.

4. Dislocation dynamics in thin films

The effect of Mg on the propagation of dislocations is particularly visible during the early stages of loading. While, in the case of pure Al, the dislocations instantly spread across the entire grain (i.e. faster than the 30 frames per second video sampling rate), they advance more slowly and in a jerky type fashion in all observed Al-Mg alloys. Fig. 2 shows a sequence of images from an indentation in Al-2.6%Mg. The arrows mark the consecutive positions where the leading dislocation line is pinned by solutes. From these images, the mean jump distance between obstacles is estimated to be of the order of 50 nm. Due to the single-tilt axis limitation of the indentation stage, the orientation of the slip plane relative to the electron beam is unknown; therefore, the measured jump distance is a projection and a lower bound of the actual jump distance.

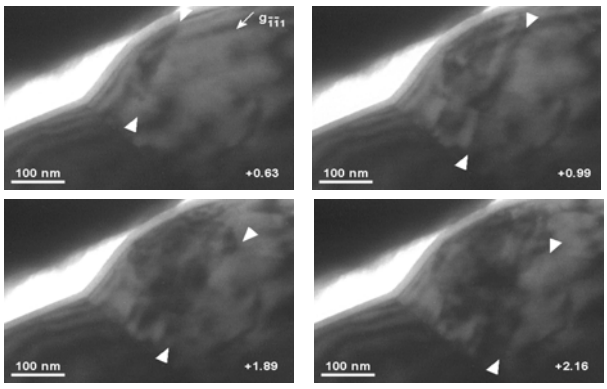

Fig. 2. Series of bright-field images showing jerky motion of dislocations during indentation of Al-2.6wt%Mg. The time from the start of the indentation is given in seconds. Note the presence of a native oxide layer on the surface [17].

At the low strains for which jerky-type dislocation motion is observed, solute atoms are the predominant barriers to mobile dislocations, as has been shown in earlier in situ pulsed nuclear magnetic resonance (NMR) experiments [1,14,15]. The mean jump distance can be predicted by Mott-Nabarro's model of weakly interacting diffuse forces between Mg solutes and dislocations in Al [9,16]. A calculation of the effective obstacle spacing, assuming that the maximum internal stress around a solute atom has a logarithmic concentration dependence, yields a value of 30 nm in Al-2.6%Mg. This is in fair agreement with our experimental observation of a mean jump distance of the order of 50 nm.

Besides solute atoms, (semi-)coherent β'/β precipitates in Al-Mg alloys can also provide significant barriers to dislocation motion. The mean spacing of these precipitates could not be measured very accurately due to the limited resolution of the microscope combined with the specific indentation stage. However, we can make an estimate based on the solid solubility of magnesium in Al at room temperature of 1.9 wt%. The calculated volume fraction f_V is 2.4 % for the β phase at 300 K. The mean planar separation, which is a relevant measure for the interaction of a gliding dislocation with a random array of obstacles in its slip plane, is given by [17]

$$\lambda \cong \frac{2\sqrt{2}\pi r}{3f_V} \tag{1}$$

provided that the size of the particles r is negligible in comparison with their center-to-center separation, i.e. if $\lambda >> r$. It is reasonable to assume that the minimum size of the semicoherent precipitates is at least 10 nm to produce sufficient strain contrast in Fig. 3. As a result, the mean planar separation of the precipitates is calculated to be at least 92 nm, i.e. larger than the mean separation between the solutes. In this approach, the obstacles are assumed to be spherical and consequently we ignore the effect that the precipitation in Al may become discontinuous or continuous depending on the temperature. However, even in the case of a Widmanstätten structure, the effective separation between the needle-shaped precipitates is larger than the effective solute obstacle spacing [18]. Therefore, based on the experimental observations in the alloys below and above the solid solubility of magnesium, the strain contrast depicted in Fig. 3 and the abovementioned theoretical considerations, solute atoms are assigned as the main obstacles to dislocation motion.

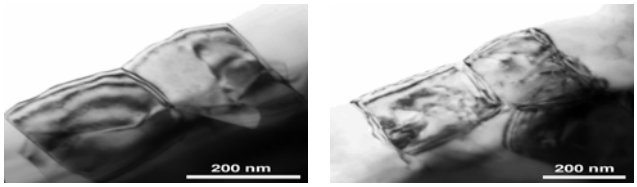

Fig. 3. Bright-field images of evaporated Al-Mg layers with (a) 1.1 and (b) 5.0 wt% Mg. The presence of Al-Mg precipitates in (b) is revealed by strain contrast.

A considerable part of previous research effort on Al-Mg alloys has been devoted to understanding the pronounced, repeated yielding that occurs during plastic deformation of these alloys. The physical basis for this phenomenon, known as the Portevin - Le Châtelier (PL) effect or serrated yielding [19], is a negative strain rate sensitivity of the flow stress, caused by interaction between dislocations and mobile solute atoms [20]. The PL effect in Al-Mg has been investigated in several deformation modes, including depth-sensing indentation [21,22]. The associated dislocation dynamics have been characterized by in situ straining in a high-voltage electron microscope [23,24] and pulsed NMR experiments [1,14,15]. In situ straining studies in a TEM have related the PL effect to sudden activation, multiplication and coordinated motion of dislocations [23,24,25]. Such behavior was not observed in our in situ experiments. Moreover, the indentation depths at which dislocation motion was studied were considerably lower than the estimated critical depths as obtained above. Therefore, it is concluded that the jerky motion observed in situ is due to solute drag without appreciable diffusion of solute Mg.

The extraction of physical properties from the quantitative indentation measurements on the evaporated thin films was compromised by the surface roughness and the grain size at shallow depths and by the film thickness at deeper depths. Recent numerical studies [26,27] suggest that for a soft film on a hard substrate, the influence of the substrate may not be appreciable until the depth exceeds one half of the film thickness. Still at these relatively high indentation depths, the probed volume was not sufficiently large to give reliable hardness and modulus data.

Analysis of the curvature of the loading portions prior to the first excursion (Fig. 4) and between subsequent excursions in the pure Al film shows that these are well described by elastic loading by a Berkovich indenter. The yield behavior is therefore classified as staircase yielding due to sudden dislocation nucleation and propagation. Staircase yielding has been reported for indentation of both single crystal and polycrystalline Al thin films [28]. The absence of these yield events during indentation of Al-Mg films, both below and above the solubility limit, shows that initial plasticity is significantly affected by solute Mg. (Fig. 4). Most likely, solute drag prevents dislocation bursts from propagating through the crystal, i.e. the stored elastic energy is insufficient to push a series of dislocations through the solute atmosphere at constant indentation load. As the load increases further, some of the available dislocations are able to overcome the force associated with solute pinning, thereby allowing plastic relaxation to proceed smoothly. Since there is no collective motion of dislocations as in pure Al, the measured loading response is essentially continuous. This perception is supported by the extensive solute drag observed in situ.

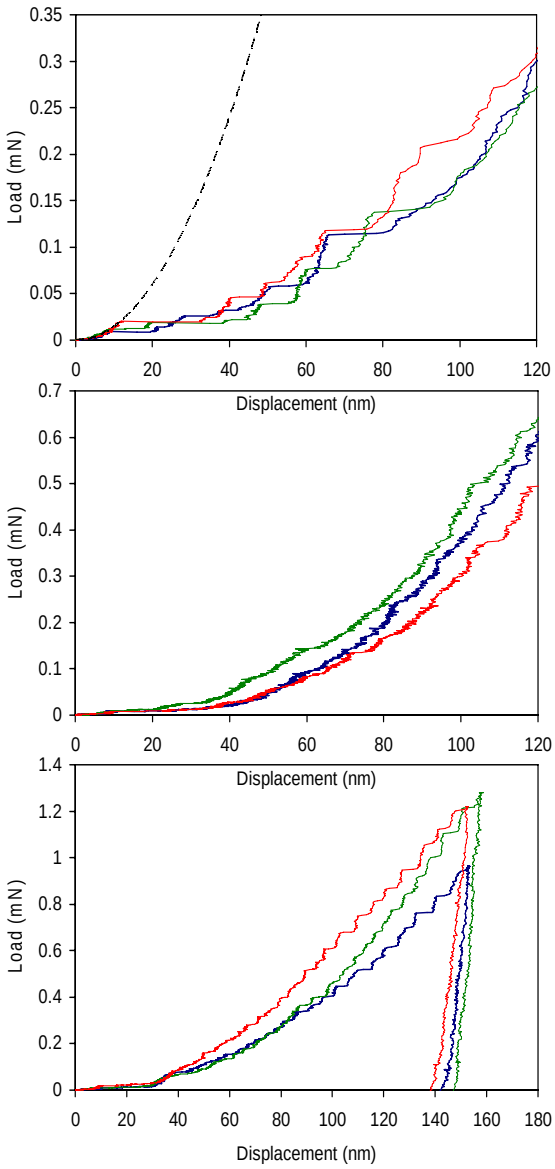

Fig. 4. Displacement-controlled indentation behavior measured in situ on (a) pure Al and (b) Al-2.6% Mg. The load drops in both materials are similar.

Interestingly, the difference in initial yield behavior between the pure Al and Al-Mg films was not observed in a quantitative displacement-controlled indentations performed in situ. The loading curve shows pronounced load drops, which have the same physical origin as the displacement excursions in load-controlled indentation, i.e. stress relaxation by bursts of dislocation activity. Also in this case, the loading behavior up to the first load drop appears to follow closely the elastic Berkovich response although this comparison may not be entirely valid because of irregularities on the tip surface as observed in TEM. The quantitative in situ indentations show a considerable amount of dislocation activity prior to the first macroscopic yield point. These observations provide strong evidence in support of the claim that dislocations are nucleated prior to the first detectable yield point in the

load-displacement curve [29-31]. The loading behavior may consequently be classified as quasi-plastic, since only limited plasticity occurs at this stage. In the present in situ experiments, the geometry of the indenter tip is not so accurately defined as to conclusively validate the correspondence of the loading curve to purely elastic loading. Furthermore, the geometry and the microstructure of the specimens may affect the nucleation behavior through the presence of nearby grain boundaries and free surfaces. To further clarify the dislocation dynamics at this initial stage of nanoindentation, in situ experiments on more carefully defined systems have recently been conducted [32].

5. Grain boundary dynamics in thin films

To confirm the occurrence of grain boundary movement in aluminum as had been reported earlier [7], several in situ indentations were performed near grain boundaries in the pure Al film. Indeed, significant grain boundary movement was observed for both low and high-angle boundaries. It should be emphasized that the observed grain boundary motion is not simply a displacement of the boundary together with the indented material as a whole; the boundary actually moves through the crystal lattice and the volume of the indented grain changes accordingly at the expense of the volume of neighboring grains (Fig. 5). The trends observed throughout the indentations suggest that grain boundary motion becomes more pronounced with decreasing grain size and decreasing distance from the indenter to the boundary. Moreover, grain boundary motion occurs less frequently as the end radius of the indenter increases due to tip blunting or contamination. Both these observations are consistent with the view that the motion of grain boundaries is promoted by high local stress gradients as put forward in the introduction of this paper. The direction of grain boundary movement can be both away from and towards the indenter, and small grains may even completely disappear under indentation. Presumably, the grain boundary parameters play an important role in the mobility of an individual boundary, since the coupling of the indenter-induced stress with the grain boundary strain field depends strongly on the particular structure of the boundary.

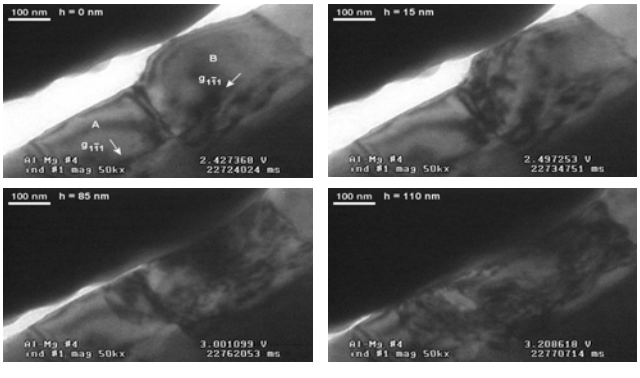

Fig. 5. Series of bright-field images from an indentation on Al-1.8% Mg. No movement of the high-angle grain boundaries is observed [17].

The quantitative in situ indentation technique offers the possibility to directly relate the observed grain boundary motion to features in the load-displacement curve. While this relationship has not been thoroughly studied in the present investigation, preliminary results suggest that the grain boundary motion is associated with softening in the loading response. Softening can physically be accounted for by the stress relaxation that occurs upon grain boundary motion. However, the quantification of overall mechanical behavior is complicated by the frequent load drops at this stage of indentation, and further in situ indentation experiments are needed to investigate this phenomenon more systematically and quantitatively.

The movement of grain boundaries as observed in Al was never found for high-angle boundaries in any of the Al-Mg specimens, even when indented to a depth greater than half of the film thickness. Fig. 6 shows a sequence of images from an indentation on an Al-1.8%Mg layer. At an indentation depth of approx. 85 nm into grain B (Fig. 6), plastic deformation is initiated in grain A by transmission across the grain boundary. However, no substantial grain boundary movement occurs; small grain boundary shifts (~ 10 nm) that were measured occasionally can be attributed to displacement of the material under the indenter as a whole, with conservation of grain volume, rather than to actual grain boundary motion. Our observations as such indicate a significant pinning effect of Mg on high-angle grain boundaries in these alloys.

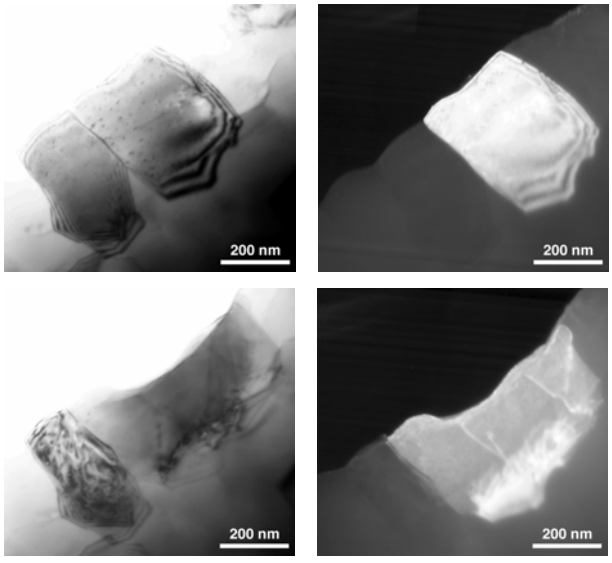

Fig. 6. Bright- and dark-field images of the indented grain (a,b) before and (c,d) after the indentation. Apart from a slight displacement of the boundaries due to the shape change of the indented grain, no significant grain boundary motion is detected.

In contrast to high-angle grain boundaries, the mobility of low-angle boundaries in Al-Mg was found to be less affected by the presence of Mg. At a relatively low indentation depth of about 20 nm, the dislocations that were initially confined to the indented grain spread across both grains without being visibly obstructed by the tilt boundary. The boundary effectively disappears at this

point with the end result of the two grains becoming one. Figs. 7a-c show the orientation of the two grains before indentation. The grains share the same <112> zone axis, but are in different two-beam conditions due to their slight misorientation (~ 0.7°). Fig. 7d shows the grains after the indentation to be both in the same diffracting condition as the grain in Fig. 7a.

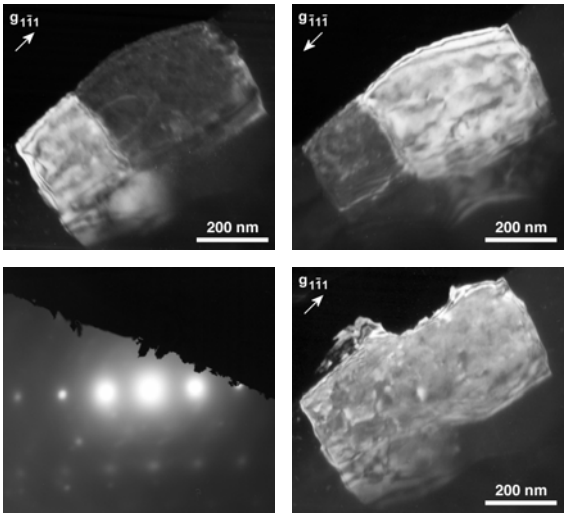

Fig. 7. (a,b) Dark-field images of the two Al-5.0%Mg grains shown in Fig. 12 before indentation. (c) Diffraction pattern showing the <112> orientation of both grains; the cut - off is due to the in situ specimen geometry. (d) Dark-field image after indentation [13].

Ideally, in order to compare the observed grain boundary behavior between different measurements, the indenter-induced stress at the boundary should be known. However, due to surface roughness, tip imperfections and the complicated specimen geometry, it is difficult to accurately measure or calculate the local stress fields. Comparisons between different measurements are therefore mainly based on indentation depth. Our observation of grain boundary pinning in Al-Mg in this context means that no motion of high-angle boundaries was observed in Al-Mg in more than fifteen indentations to a depth of the order of 100 nm, while in pure Al, grain boundary motion was frequently observed at indentation depths of 50 nm or less.

The Al-Mg films used in this study include compositions both below and above the solubility limit of Mg in Al. However, no differences in indentation behavior between the solid solution and the precipitated microstructures were observed. Consequently, the observed pinning of high-angle boundaries in Al-Mg is attributed to solute Mg. The pinning is presumably due to a change in grain boundary structure or strain fields caused by solute Mg atoms on the grain boundaries. Relatively few direct experimental observations have been reported on this type of interaction. Sass and co-workers observed that the addition of Au and Sb impurities to bcc Fe changes the dislocation structure of <100> twist boundaries of both low-angle [33] and high-angle [34] misorientation. Rittner and Seidman [35] calculated solute distributions at <110> symmetric tilt boundaries with different boundary structures in an fcc binary alloy using atomistic simulations. However, the influence of solutes on the structure of such boundaries has not been experimentally identified.

Possible changes in atomic boundary structure due to solute atoms may be observed by high-resolution TEM (HRTEM). Atomic-scale observation of grain boundaries using this technique requires that the crystals on both sides share a close-packed direction so that both lattices can be atomically resolved at the same time. The mazed bicrystal structure that forms when an Al film is deposited epitaxially onto a Si (001) surface meets this condition. The epitaxial relationships Al (110) // Si (001), Al [001] // Si [110] and Al (110) // Si (001), Al [001] // Si $[1\bar{1}0]$ lead to two possible orientations that are separated exclusively by 90° <110> tilt boundaries [13,36]. The structure of such boundaries has been successfully studied in HRTEM studies of Al films on Si substrates [13,37,38] and Au films on Ge substrates [39-42], which exhibit the same epitaxial relationships. Moreover, the effect of alloying elements in Al has been explored by evaporating alloys such as Al-Cu and Al-Ag [43].

In order to study the effect of Mg on these tilt boundaries, we deposited Al and Al-Mg films onto Si (001) substrates that had been stripped of their native oxide film. Indeed, we found that in epitaxial films evaporated from pure Al, the 90° <110> tilt grain boundaries are facetted on $\{100\}_A//\{110\}_B$ and $\{557\}_A//\{557\}_B$ planes, which can be atomically resolved (Fig. 8a). The addition of Mg however drastically changes the microstructure of the deposited film: evaporation of Al-Mg on a Si substrate heated to 300 °C (which is necessary to reduce the lattice mismatch between Al and Si) leads to the formation of the intermetallic compound Mg_2Si, which prohibits any further epitaxial growth (Fig. 8b). Even in a two-step evaporation consisting of a pure Al deposition to provide a basis for the bicrystal structure and a subsequent Al-Mg deposition to introduce the Mg, the Mg diffuses to the substrate, driven by the reaction with the Si substrate. This method therefore could not be used to study the effect of Mg on the atomic structure of the grain boundaries.

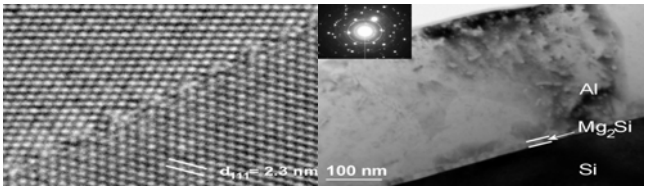

Fig. 8. (a) High-resolution micrograph of a 90° <110> asymmetrical tilt boundary in an epitaxial Al thin film, showing a periodic structure along the boundary plane. The orientation of the boundary plane is $\{100\}_A//\{110\}_B$. (b) Cross section of a film deposited from an Al-2.2wt%Mg source onto a Si (001) substrate; the intermetallic compound Mg_2Si, identified by its diffraction ring pattern (inset), forms a 15 nm thick layer at the interface.

Another effect that may contribute to the pinning of special boundaries is solute drag on extrinsic grain boundary dislocations (EGBDs) as reported by Song et al. [44], who showed that the dissociation rate of EGBDs in Al alloys is reduced by the addition of Mg. This implies that the indenter-induced deformation is accommodated more easily by these boundaries in pure Al than by those in Al-Mg.

The fact that low-angle grain boundaries were found to be mobile regardless of the Mg content can be explained by their different boundary structure. Up to a misorientation of 10-15°, low-angle boundaries can be described as a periodic array of edge and screw dislocations by Frank's rule [45]. In such an arrangement, the strain fields of the dislocations are approximated well by individual isolated dislocations and their interaction with an external stress field can be calculated accordingly. Since there is no significant interaction between the individual grain boundary dislocations, the stress required to move a low-angle boundary is much lower than for a high-angle boundary. Low-angle pure tilt boundaries consisting entirely of parallel edge dislocations are fully glissile and therefore particularly mobile. In general, a combination of glide and climb is required to move a low-angle boundary [46].

As a corollary, the structural difference between low and high-angle boundaries also affects the extent of solute segregation. Because solutes generally segregate more strongly to high-angle boundaries [47], the observed difference in mobility may partly be a compositional effect.

6. Conclusions

The experiments presented provide insights into the nano-physical behavior of Al and Al-Mg alloys at room temperature by making use of in situ nanoindentation in a TEM. The observed propagation of dislocations is markedly different between Al and Al-Mg films: the presence of solute Mg results in solute drag, evidenced by jerky dislocation motion with a mean jump distance that compares well to earlier theoretical and experimental results. It is proposed that this solute drag accounts for the difference in load-controlled indentation response between Al and Al-Mg alloys. Several yield excursions are observed during initial indentation of pure Al, which are commonly attributed to collective motion of dislocations nucleated under the indenter. These yield excursions are attenuated during indentation of the Al-Mg alloys; presumably, the solute drag prevents the elastic energy from being released in a sudden dislocation burst and thus smoothes out the initial indentation response. Displacement-controlled indentation does not result in a qualitative difference between Al and Al-Mg, which can be explained by the specific feedback characteristics providing a more sensitive detection of plastic instabilities and allowing the natural process of load relaxation to occur.

The in situ indentation measurements confirm grain boundary motion as an important deformation mechanism in ultrafine-grained Al when it is subjected to a highly inhomogeneous stress field as produced by a Berkovich indenter. It is found that solute Mg effectively pins high-angle grain boundaries during such deformation. The proposed mechanism for this pinning is a change in the atomic structure of the boundaries, possibly aided by solute drag on extrinsic grain boundary dislocations. The mobility of low-angle boundaries is not affected by the presence of Mg, which is attributed to their different boundary structure consisting of periodic dislocation arrangements.

Acknowledgements

The work was part of the research program of the Netherlands Institute for Metals Research, project nr MC4.01104. The paper summarizes the work in collaboration with Andy M. Minor, Steven Shan, Eric A. Stach, all from LBL Berkeley USA, and with S.A. Syed Asif (Hysitron) and Oden L. Warren (Hysitron).

References

[1] J. Th. M. De Hosson, O. Kanert, A. W. Sleeswyk, in: Dislocations in Solids, Vol. 6, ed. F. R. N. Nabarro (North-Holland, Amsterdam, 1983), 441.
[2] M. A. Wall, U. Dahmen, Microsc. Microanal. **3**, 593 (1997).
[3] M. A. Wall, U. Dahmen, Microsc. Res. Tech. **42**, 248 (1998).
[4] E. A. Stach, T. Freeman, A. M. Minor, D. K. Owen, J. Cumings, M. A. Wall, T. Chraska, R. Hull, J.W. Morris, Jr., A. Zettl, U. Dahmen, Microsc. Microanal. **7**, 507 (2001).
[5] A. M. Minor, J. W. Morris, Jr., E. A. Stach, Appl. Phys. Lett. **79**, 1625 (2001).
[6] A. M. Minor, E. T. Lilleodden, E. A. Stach, J. W. Morris, Jr., J. Electron. Mater. **31**, 958 (2002).
[7] A. M. Minor, E. T. Lilleodden, E. A. Stach, J. W. Morris, Jr., J. Mater. Res. **19**, 176 (2004).
[8] W. A. Soer, J. Th. M. De Hosson, A. M. Minor, E. A. Stach, J. W. Morris Jr., Mater. Res. Soc. Symp. Proc. **795**, U9.3.1 (2004).
[9] W. A. Soer, J. Th. M. De Hosson, A. M. Minor, J. W. Morris Jr., E. A. Stach, Acta Mater. **52**, 5783 (2004).
[10] A. M. Minor, Ph. D. thesis (University of California, Berkeley, 2002).
[11] O. L. Warren, S. A. Downs, T. J. Wyrobek, Z. Metallkd. **95**, 287 (2004).
[12] L. F. Mondolfo, Aluminum Alloys: Structure and Properties (Butterworth, London, 1979), 313.
[13] U. Dahmen, K. H. Westmacott, Scripta Metall. **22**, 1673 (1988).
[14] U. Schlagowski, O. Kanert, J. Th. M. De Hosson, G. Boom, Acta Metall. **36**, 865 (1988).
[15] J. Th. M. De Hosson, O. Kanert, U. Schlagowski, G. Boom, J. Mater. Res. **3**, 645 (1988).
[16] F. R. N. Nabarro, in: The Physics of Metals, Vol. 2, ed. P.B. Hirsch (Cambridge University Press, 1975), 152.

[17] A. J. E. Foreman, M. J. Makin, Philos. Mag. **14**, 911 (1966).
[18] J. Th. M. De Hosson, W. H. M. Alsem, H. Tamler, O. Kanert, in: Defects, Fracture and Fatigue, eds. G.C. Sih, J.W. Provan (Martinus Nijhoff, The Hague, 1983), 23.
[19] P. G. McCormick, Acta Metall. **20**, 351 (1972).
[20] A. van den Beukel, Acta Metall. **28**, 965 (1980).
[21] G. Bérces, N. Q. Chinh, A. Juh´asz, J. Lendvai, J. Mater. Res. **13**, 1411 (1998).
[22] N. Q. Chinh, F. Csikor, Zs. Kova´cs, J. Lendvai, J. Mater. Res. **15**, 1037 (2000).
[23] T. Tabata, H. Fujita, Y. Nakajima, Acta Metall. **28**, 795 (1980).
[24] J. M. Robinson, Mater. Sci. Eng. A **203**, 238 (1995).
[25] L. P. Kubin, Y. Estrin, Acta Metall. Mater. **38**, 697 (1990).
[26] X. Chen, J. J. Vlassak, J. Mater. Res. **16**, 2974 (2001).
[27] Z. H. Xu, D. Rowcliffe, Thin Solid Films **447-448**, 399 (2004).
[28] A. Gouldstone, H.-J. Koh, K.-Y. Zeng, A.E. Giannakopoulos, S. Suresh, Acta Mater. **48**, 2277 (2000).
[29] W. W. Gerberich, S. K. Venkataraman, H. Huang, S. E. Harvey, D. L. Kohlstedt, Acta Metall. Mater. **43**, 1569 (1995).
[30] W. W. Gerberich, J. C. Nelson, E. T. Lilleodden, P. Anderson, J. T. Wyrobek, Acta Mater. **44**, 3585 (1996).
[31] D. F. Bahr, D. E. Kramer, W. W. Gerberich, Acta Mater. **46**, 3605 (1998).
[32] A. M. Minor, S. A. Syed Asif, Z. Shan, E. A. Stach, E. Cyrankowski, T. J. Wyrobek, O. L. Warren, submitted.
[33] K. Sickafus, S. L. Sass, Scripta Metall. **18**, 165 (1984).
[34] C. H. Lin, S. L. Sass, Scripta Metall. **22**, 735 (1988).
[35] J. D. Rittner, D. N. Seidman, Acta Mater **45**, 3191 (1997).
[36] F. J. Lamelas, M.-T. Tang, K. Evans-Lutterodt, P. H. Fuoss, W. L. Brown, Phys. Rev. B **46**, 15570 (1992).
[37] U. Dahmen, C. J. D. Hetherington, M. A. O'Keefe, K. H. Westmacott, M. J. Mills, M. S. Daw, V. Vitek, Philos. Mag. Lett. **62**, 327 (1990).
[38] S. Paciornik, R. Kilaas, J. Turner, U. Dahmen, Ultramicroscopy **62**, 15 (1996).
[39] J. M. Pénisson, F. Lançon, U. Dahmen, Mater. Sci. Forum 294-296, 27 (1999).
[40] K. L. Merkle, L. J. Thompson, Phys. Rev. Lett. **83**, 556 (1999).
[41] D. L. Medlin, S. M. Foiles, D. Cohen, Acta Mater. **49**, 3689 (2001).
[42] D. L. Medlin, D. Cohen, R. C. Pond, Philos. Mag. Lett. **83**, 223 (2003).
[43] K. H. Westmacott, S. Hinderberger, U. Dahmen, Philos. Mag. A **81**, 1547 (2001).
[44] S. G. Song, J. S. Vetrano, S. M. Bruemmer, Mater. Sci. Eng. A **232**, 23 (1997).
[45] F. C. Frank, in: A Symposium on the Plastic Deformation of Crystalline Solids (Office of Naval Research, Washington, DC, 1950), 151.
[46] W. T. Read, Dislocations in Crystals (McGraw-Hill, New York, 1953).
[47] A. P. Sutton, R. W. Balluffi, Interfaces in Crystalline Solids (Clarendon Press, Oxford, 1995).

*Corresponding author: j.t.m.de.hosson@rug.nl